XH defects in nonmetallic solids: Isotope effects and anharmonicities as probes of the defect environment

W. Beall Fowler
Department of Physics and Sherman Fairchild Laboratory, Lehigh University, Bethlehem, Pennsylvania 18015

R. Capelletti and E. Colombi
Dipartimento di Fisica dell'Università, Viale delle Scienze, 43100 Parma, Italy
(Received 24 September 1990; revised manuscript received 7 February 1991)

We have developed a technique to analyze the ir stretch modes of XH defects in nonmetallic solids, where X is an atom or ion heavier than hydrogen. This technique draws heavily upon molecular theory: The XH defect is treated by a Morse potential modified by coupling of X to the lattice with use of a one-dimensional model. The electrical anharmonicity of the dipole moment is included in obtaining transition strengths. The importance of overtone data as well as deuteration is demonstrated. A number of systems involving OH^- in insulating solids are analyzed. These include (1) OH^-, OD^-, and OT^- in TiO_2 [J. B. Bates and R. A. Perkins, Phys. Rev. B **16**, 3713 (1977)]; (2) OH^- and OD^- in Mg-doped LiF and NaF [R. Capelletti *et al.*, Cryst. Latt. Defects Amorph. Mater. **16**, 189 (1987)]; (3) OH^- and OD^- in $LiNbO_3$ [A. Forster *et al.*, Phys. Status Solidi B **143**, 755 (1987)]; and (4) OH^- and OD^- in CsCl and CsBr [M. Krantz and F. Luty, Phys. Rev. B **37**, 7038 (1988)]. The defects in TiO_2 exhibit a surprisingly large mechanical anharmonicity. The data on Mg-doped fluorides indicate electrical anharmonicities which in some cases are considerably different from that of molecular OH^-.

I. INTRODUCTION

Study of the infrared properties of hydrogen-related defects in semiconductors and insulators has been a significant tool in obtaining information about the structures and properties of such defects.[1–4] Hydrogen is a particularly important defect constituent because of its frequent occurrence, its small size and mass, the existence of several isotopes, and its ability to form several types of chemical bonds. In most nonmetallic solids, hydrogen-related stretching bands and their combination and overtone bands lie well above the vibrational bands of the host, thus making them amenable to conventional ir spectroscopic techniques.

In this paper we investigate some of the theoretical aspects of the ir spectra of hydrogen-related defects, using OH^- in insulating crystals as an example. We show that it is possible to extract considerable information from ir stretching bands if one can vary the isotope and the temperature and if the positions and strengths of both fundamental and overtone bands can be measured. Electrical anharmonicity is found to be significant, as it is indeed known to be in other hydrogen-related systems.

An important early example of this type of analysis is contained in the paper of Bates and Perkins[5] (BP) on OH^- in TiO_2. BP measured the ir spectra of OH^-, OD^-, and OT^- at temperatures ranging from 8 to 300 K. They analyzed their measured isotopic frequency shifts and intensities on the basis of two models, a diatomic anharmonic oscillator model and a harmonic hydrogen-bonded model. Based on this analysis, they concluded that the hydrogen-bonded model was inconsistent with experiment.

We extended the BP model[6] and applied our version to data obtained for Ti- and Mg-related OH^- and OD^- centers in LiF. Here, too, the anharmonic oscillator model seems basically correct. However, there is striking evidence for electrical anharmonicity (nonlinearity of the electric dipole moment with O-H separation), in addition to mechanical anharmonicity, in certain of the complex defects studied in LiF. This electrical anharmonicity and its temperature dependence may indicate defect-host interactions not previously considered.

In this paper the theoretical aspects of the approach used to analyze the data of Ref. 6 are discussed. The importance of the coupling of the defect molecule to the lattice through the O atom, and its effect on isotope shifts, is demonstrated. Further analysis of the data of BP suggests an anomalously large anharmonic contribution to the internal OH^- stretching mode, which, at the present time, cannot be explained. The effects of the electrical anharmonicity are considered in detail and are applied to defects in LiF and NaF. Published data on OH^- and OD^- in $LiNbO_3$ and in cesium halides are briefly considered.

II. THEORY

A. Model for analysis

We treat OH^- as an anharmonic diatomic molecule coupled harmonically through O to the lattice. This is similar to a number of successful treatments of XH in molecules (where in many cases X is carbon).[7–10] This type of approach works well for molecules, even for highly excited local modes. One may understand why this is

the case by considering a model problem, namely, a light atom (m) at the end of a semi-infinite chain coupled harmonically to heavier atoms. In the simplest version, all atoms but the light one are identical (M) and all force constants are identical (k). As shown in the Appendix, one may then use a recursion method to demonstrate that, in the expression for the local-mode frequency

$$\omega=(k/\mu)^{1/2} , \tag{1}$$

the reduced mass μ is given exactly by

$$\mu=m(1-m/M) . \tag{2}$$

It is important to note that the exact reduced mass agrees to first order with the reduced mass of the free diatomic oscillator. For example, if $m=1$ and $M=16$, the exact reduced mass [Eq. (2)] equals 0.9375, while the diatomic reduced mass equals 0.9412. This is only a 0.4% difference. A similar correspondence between the exact result and a diatomic result may be noted in a detailed vibrational calculation of H attached to Si which is attached to a silicon Bethe lattice.[11]

One may modify the one-dimensional chain by introducing different masses and force constants, and, indeed, we have done so in the calculations discussed below. But it is important to emphasize the basic result: to an excellent first approximation, one may treat the stretching vibration of XH attached through X to other atoms as the vibration of a free diatomic XH molecule.

There are several possible ways to include refinements to the free diatomic model. Newman and co-workers[12,13] have modified the diatomic reduced mass by multiplying the heavier mass by a factor. Very recently Dumas, Chabal, and Higashi[14] have reported an extensive study and analysis of H attached to a Si atom at a silicon (111) surface. They find evidence of anharmonic coupling to silicon phonons. Hutchinson, Reinhardt, and Hynes[8] analyzed energy transfer in a H—C—C—C—$\cdots$ chain by using a Morse potential[15] for H—C and harmonic potentials for C—C. They used the normal modes for the harmonic problem to construct the potential for the actual vibration. In this way, their potential energy included all the "springs" in the system (although only the Morse potential and the nearest-neighbor spring participate in a non-negligible way).

We have chosen a correction somewhat different from that of Hutchinson, Reinhardt, and Hynes. Namely, we treat the XH system as a Morse oscillator, but with a reduced mass appropriate to the harmonic system X-H plus linear chain. [In the simplest case, then, the mass would be that given in Eq. (2).] Neither our approach nor that of Hutchinson, Reinhardt, and Hynes is exact, but as small corrections to the Morse problem, they are likely to be equally useful in a data-fitting sense. For example, the small harmonic energy associated with the nearest-neighbor spring in the approach of Hutchinson, Reinhardt, and Hynes would be included in the Morse oscillator in our approach.

B. The Morse oscillator

The Morse potential[15] may be written as

$$U(r-r_e)=D_e\{1-\exp[-\beta(r-r_e)]\}^2 , \tag{3}$$

where r_e is the equilibrium separation and D_e and β are constants. The exact solution of the Schrödinger equation[15] yields term values $G(n)$ given by

$$G(n)=\omega_e(n+\tfrac{1}{2})-\omega_e x_e(n+\tfrac{1}{2})^2 , \tag{4}$$

where

$$\omega_e=\beta(\hbar D_e/\pi c\mu)^{1/2} , \tag{5}$$

$$\omega_e x_e=\hbar\beta^2/4\pi c\mu , \tag{6}$$

and μ is the reduced mass of the system. We note that $G(n)$ depends on both potential and kinetic energies.

The transition wave number is given by

$$\Delta G_{n0}=G(n)-G(0)=n\omega_e[1-x_e(n+1)] . \tag{7}$$

We consider the fundamental and the first overtone, and define a ratio R_{ov} by

$$R_{ov}=\Delta G_{20}/2\Delta G_{10}=(1-3x_e)/(1-2x_e) , \tag{8}$$

so measurements of both the fundamental and first overtone allow a determination of both ω_e and x_e.

Furthermore, measurements of these wave numbers for different isotopes yield ratios of the reduced masses for those isotopes which can then be analyzed by force-constant models. For example, defining ρ as the ratio between reduced mass for the XH system to that for the XD system,

$$\Delta G_{10}^{D}/\Delta G_{10}^{H}=\rho^{1/2}(1-2\rho^{1/2}x_e^{H})/(1-2x_e^{H}) . \tag{9}$$

C. Transition probabilities

For a purely harmonic potential and an electric-dipole moment proportional to the X-H separation, there will be no overtone absorption. Thus, the intensity I from 0 to 2, I_{02}, will be zero. However, for a Morse potential (or for other anharmonic corrections to the harmonic potential) there can be absorption to the overtones. For a Morse potential and an electric-dipole moment proportional to the X-H separation, the ratio of the overtone to the fundamental absorption strength is given by[16]

$$I_{02}/I_{01}=x_e(1-5x_e)/(1-3x_e)^2\approx x_e . \tag{10}$$

Thus, one would expect the ratio of transition strengths to be of order a few hundredths in most cases. It has been recognized, however, that in free diatomic systems such ratios often differ greatly from the value x_e because the assumption that the dipole moment is proportional to the X-H separation is often seriously flawed.

The nonlinearity of the electric-dipole moment with separation is called *electrical anharmonicity* and has been extensively studied. Detailed *ab initio* calculations of dipole moments confirm such nonlinearities.[17,18] These nonlinearities may be included in analyses such as ours in several ways. First, one may compute the electric-dipole matrix elements using the Morse wave functions and the computed dipole moment variation. Second, one may expand the computed dipole moment in a power series about the equilibrium position and include the higher-order terms in computing the transition-matrix ele-

ments.[19] Third, one may use an analytical fit to the dipole moment expression $M(r)$ of the form

$$M(r)=kr\exp(-r/r^*)\ , \tag{11}$$

where the constants k and r^* are chosen to fit the computed dipole moment. This expression allows for covalency in the bond and approaches reasonable limits for small and large r (to within an unimportant constant). Furthermore, it has the practical advantage that matrix elements of Eq. (11) with respect to Morse potential eigenfunctions may be evaluated analytically, as demonstrated by Sage.[20]

D. Further theoretical considerations

The preceding sections outlined major theoretical concepts which are utilized in analyzing ir data on various OH^- examples in the remainder of this paper. As the data are presented, other notions will be considered. These include possible anharmonicities associated with the interaction of O with its nonhydrogen neighbors.

As for a second possibility, hydrogen bonding, while we have considered this to some degree, we will discuss it only briefly. There simply seems to be little evidence[5] for "conventional" hydrogen bonding to be a significant factor in the defects which we consider in this paper. This contrasts with certain hydrogen-related defects in other systems; for example, interstitial H in silicon has an equilibrium bond-centered position, where it interacts strongly with two silicons.[21] The E_4' center in α-quartz[22] is a hydrogen substituted for an oxygen: again, the hydrogen interacts strongly with two silicons. In both of these examples the hydrogen-silicon distances are close and the potentials are double well. The defects considered herein are quite different.

III. EXAMPLES

A. Bates and Perkins data on OH^-, OD^-, OT^- in TiO_2

Bates and Perkins[5] measured the stretching bands of OH^-, OD^-, and OT^- in TiO_2 at 300, 77, and 8 K. They analyzed their data successfully using a two-term anharmonic oscillator model. An analysis using a harmonic hydrogen-bonded model did not agree with results based on known H-bonded systems.

Their data were restricted to the fundamental bands; they measured no overtones. Therefore, the determination of ω_e and x_e requires the isotope data and a force-constant model. We use

$$\Delta G_{10}=\omega_e(1-2x_e) \tag{12}$$

with ω_e and x_e each proportional to $\mu^{-1/2}$. Table I gives wave number data taken from Table I of BP.

With the reduced-mass ratios for isolated OH^-, the ratio $\Delta G^{OD}/\Delta G^{OH}$ yields a value $x_e^H=0.038$ for OH^-. The same procedure with ΔG^{OT} also yields the same value for x_e^H. This value persists for the data at all three temperatures to within 2%.

TABLE I. Wave numbers (in cm^{-1}) for OH^-, OD^-, and OT^- bands in TiO_2, determined experimentally by Bates and Perkins (Ref. 5), and calculated values of ω_e^H (in cm^{-1}), x_e^H, and the O-lattice force constant k_{OL} (as a fraction of the O-H value), which provide best fits to the data.

T (K)	300	77	8
OH^-	3276	3286	3286.5
OD^-	2437	2445	2445
OT^-	2065	2071	2070.5
ω_e^H	3537.3	3556.2	3557.0
x_e^H	0.0370	0.0380	0.0379
k_{OL}	0.15	0.05	0.01

Repeating the calculation but using the reduced-mass ratios for coupling through oxygen [the simplest version, Eq. (2)], we find that $\Delta G^{OD}/\Delta G^{OH}$ yields $x_e^H=0.029$, while $\Delta G^{OT}/\Delta G^{OH}$ yields $x_e^H=0.020$. Since these do not agree, we conclude that the coupling through the oxygen is weak and that $x_e^H=0.038$. We have tested this conclusion with many different simulations of oxygen couplings to the lattice and find that the best fit to the data occurs with an O-to-lattice spring constant of order 1–10% that of O—H. Table I includes the results of such a fit.

This value of x_e^H seems anomalously large. In nearly every example for which we have found data for OH^- in solids, x_e^H is found to equal 0.02, to within 10–15%. In no other case does it exceed 0.03. We have considered the possible effect of anharmonic coupling between O and the lattice. We conclude that this cannot be the source of the large anharmonicity; such a correction will be of order x_e^H times $(m_H/M_O)^4$, orders of magnitude too small.[23] It is unfortunate that BP did not measure the overtone absorption, since this would give an alternative (and more direct) determination of x_e^H. Their value of x_e^H would predict ΔG_{20} to lie at 6303 cm^{-1} [Eq. (8)], while, if x_e^H were 0.020, ΔG_{20} would be predicted to lie at 6436 cm^{-1}.

B. OH^- and OD^- in LiF:Mg and NaF:Mg: Positions

Capelletti and co-workers have carried out extensive ir measurements on OH^- and OD^- in Mg- and Ti-doped LiF and NaF. Some of their results have been published,[6] and more detailed results will follow in subsequent publications. Many OH^- lines are found; for example, in LiF:Mg, some 15 bands are observed. Detailed defect models have yet to be extracted from these data. One would imagine that two fundamental defects exist: Fig. 1 shows two possible nearest-neighbor configurations of Mg^{2+}, OH^-, and an alkali vacancy (Li^+ in the case shown). It is also clear that there could exist many non-nearest-neighbor configurations of these three defects, each perturbing the OH^- stretching mode in a slightly different way. Experiments involving different Mg concentrations provide evidence of Mg-vacancy clustering near the OH^-.

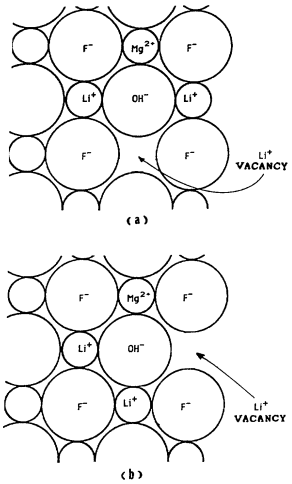

FIG. 1. Two possible configurations for an OH^- defect in LiF:Mg. (a) and (b) differ in the relative location of the Li^+ vacancy.

Table II contains some recent data and our analysis. (It should be noted that similar data in Ref. 6 were uncorrected for wavelength calibration.) The 3575-cm^{-1} band is dominant and may involve Mg-vacancy clustering. Shown are the positions ΔG_{10} and ΔG_{20} for OH^- and ΔG_{10}^{D} for OD^- measured at 9 K. The parameters ω_e^H and x_e^H are calculated from Eqs. (7) and (8) and the OH^-- to OD^--reduced-mass ratio ρ from Eq. (9).

We note from Table II that, for the seven defects considered, the average value of x_e is 0.022, with a maximum variation less than 10%. The average value of ρ is 0.531, with a maximum variation less than 0.2%. For free diatomic OH^- and OD^-, $\rho=0.529$, while for the simplest linear coupling [Eq. (2)], $\rho=0.536$. A variant of the model leading to Eq. (2), in which the mass nearest the oxygen is that of Mg, yields $\rho=0.535$. If the mass nearest the oxygen is that of Mg and the O-Mg spring constant is $\frac{1}{3}$ that of O-H, we obtain $\rho=0.531$, a value close to those obtained from experiment. Such a value of the O-Mg spring constant is approximately consistent with data on diatomic MgO.[24] If we consider each band in Table II and fit it to the linear chain model which includes a Mg next-neighbor and a variable Mg-O force constant, we can fit with high accuracy the values of ρ, x_e, and ω_e with the Mg-O force constants shown which range from 17% to 45% that of O-H. It should be noted that the O-H vibrational parameters are not very sensitive to small changes in the Mg-O force constant. It should also be noted that there is no certainty that, in each case, the OH^- is a nearest neighbor of Mg^{2+} and, in fact, the wide variation in force constants may reflect substantial differences in the detailed defect structure. The linear chain model may be particularly appropriate for those OH^- defects involving an adjacent vacancy.

Table III contains data on four of many bands studied in NaF:Mg:OH.[25] These bands, labeled *A*, *C*, *D*, and *F*, have been measured at a range of temperatures from 9 K to room temperature. The *A* band, like the 3575-cm^{-1} band in LiF:Mg:OH, is dominant and there is evidence that it involves Mg-vacancy clustering. Many of the comments made above with regard to the bands observed in LiF are also appropriate here. It may be noted, however, that the range of O-lattice couplings seen in NaF is somewhat greater than deduced for the defects in LiF. In particular, we note that line *D* is weakly coupled to the lattice while line *F* is rather strongly coupled, with *A* and *C* intermediate. Different Mg-O force constants in LiF and NaF should not be surprising; in NaF the Mg^{2+} ion is smaller than the Na^+ which it replaces and may bond more weakly to its neighbors than in LiF.

C. OH^- and OD^- in LiF:Mg and NaF:Mg: Transition strengths

As noted in Sec. II, electrical anharmonicity is expected to be of significance in many *X*H systems. To investigate this, we have measured room-temperature transition strengths, particularly the ratio of overtone to fundamental which is expected to be most sensitive to electrical anharmonicity. Measurements of transition strengths at lower temperatures are underway and will be discussed in a subsequent publication. We note that, for most of the defects which we have studied in LiF:Mg and NaF:Mg, the anharmonicity parameter x_e^H for OH^- is approximately 0.02, and since the overtone-to-fundamental transition strength ratio I_{02}/I_{01} is approximately equal to x_e

TABLE II. Wave numbers (in cm^{-1}) for the OH^- fundamental ΔG_{10} and harmonic ΔG_{20} and the OD^- fundamental ΔG_{10}^{D}, determined experimentally, and calculated values of ω_e^H (in cm^{-1}) from Eq. (7), x_e^H from Eq. (8), and ρ from Eq. (9), for several ir bands in LiF:Mg. Also listed are values of k_{OL}, the O-lattice force constant (as a fraction of the O-H value), which provide best fits to the data.

ΔG_{10}	ΔG_{20}	ΔG_{10}^{D}	ω_e^H	$100x_e^H$	ρ	k_{OL}
3575	6976.4	2637.6	3749	2.316	0.5302	0.17
3586	7002.8	2645.1	3755	2.253	0.5304	0.20
3596	7032	2653.1	3756	2.130	0.5314	0.40
3618	7085.1	2668.1	3769	2.002	0.5318	0.45
3627.5	7093.2	2676.1	3789	2.135	0.5313	0.37
3635	7106.3	2680.1	3799	2.155	0.5306	0.23
3640	7115.4	2683.6	3805	2.163	0.5304	0.21

TABLE III. Wave numbers (in cm^{-1}) for the OH^- fundamental ΔG_{10} and harmonic ΔG_{20} and the OD^- fundamental ΔG_{10}^D, determined experimentally, and calculated values of ω_e^H (in cm^{-1}) from Eq. (7), x_e^H from Eq. (8), and ρ from Eq. (9), for several ir bands in NaF:Mg. Also listed are values of k_{OL}, the O-lattice force constant (as a fraction of the O-H value), which provide best fits to the data.

Band (K)	ΔG_{10}	ΔG_{20}	ΔG_{10}^D	ω_e^H	$100x_e^H$	ρ	k_{OL}
A (9)	3592.7	7018.8	2651.2	3759.3	2.216	0.5311	0.336
A (300)	3592.7	7018.6	2651.2	3759.5	2.218	0.5311	0.336
C (9)	3609.2	7055.9	2664.2	3771.7	2.154	0.5318	0.468
C (300)	3606.9	7051.3	2661.3	3769.4	2.156	0.5313	0.378
D (9)	3625.3	7070.6	2675.2	3805.3	2.365	0.5301	0.147
D (300)	3621.3	7065.1	2672.2	3798.8	2.336	0.5303	0.180
F (9)	3635.3	7089.7	2691.6	3816.2	2.370	0.5338	0.784
F (300)	3630.3	7082.7	2685.7	3808.2	2.336	0.5331	0.678

for a Morse potential with an electric-dipole moment proportional to separation [Eq. (10)], we look for significant deviations in I_{02}/I_{01} from 0.02. (For OD^-, x_e^D would be approximately 0.014, and one would look for deviations from that value.)

As shown elsewhere,[6] we have studied several bands in LiF:Mg. Deviations in absolute values of I_{02}/I_{01} from x_e^H are found to be as large as a factor of 2. Similar results measured at room temperature for bands *A*, *C*, *D*, and *F* in NaF:Mg are shown in Table IV. These results are striking: the ratio I_{02}/I_{01} for band *A* is more than twice as large x_e^H, for band *F* the ratio is more than three times as large as x_e^H, and for bands *C* and *D*, the ratio is slightly smaller than x_e^H.

We have analyzed the transition strengths in two ways. First, we have used the computed dipole moment versus the separation of Werner, Rosmus, and Reinsch[17] and have numerically obtained the dipole matrix elements with respect to eigenfunctions of Morse potentials whose parameters are consistent with the term values and reduced masses used to fit the positions of the various bands. This is a model, then, in which different defects are taken to have slightly different potentials and wave functions, but the same dipole moment operators. As we shall see, this is not an adequate approximation in some cases.

Second, we have used the results of Sage[20] in two ways. First, we have fitted his expression [Eq. (11)] for the dipole moment to that computed by Werner, Rosmus, and Reinsch and then used his formalism to obtain dipole matrix elements. This was done primarily as a consistency check. Second, we have explored just what variations in Sage's parameters might be required to achieve agreement with experiment.

The Sage expression [Eq. (11)] does not fit the computed dipole moment particularly well over a large range of separation. One must therefore make some judgments as to which region is most important. It turns out, as we shall see, that the dipole moment of Werner, Rosmus, and Reinsch is such that the predicted ratio I_{02}/I_{01} is small and is very sensitive to small changes in the dipole moment. Thus, the fitting of the Sage expression is not likely to yield excellent quantitative agreement with the ratio predicted with the moment of Werner, Rosmus, and Reinsch, but, in fact, small changes in the Sage parameters do yield agreement with the "better" theory.

Of greater significance, the intensity ratios predicted with the dipole moment of Werner, Rosmus, and Reinsch do not agree well with experiment in many of the cases considered here. The predicted values are less than the experimental values for bands *A*–*F* in NaF:Mg by from 1–2 orders of magnitude. In order to achieve agreement, we may use the Sage expression and vary the parameter r^*. Whereas a value of r^* in the region 0.65–0.7 Å yields a fair fit to the dipole moment of Werner, Rosmus, and Reinsch (agreement with their computed intensity ratio for free OH^- is found for $r^*=0.703$ Å), we find that a value of r^* in the region 0.8–0.9 Å is needed to obtain intensity ratios consistent with experiment for bands *A*–*F* in NaF:Mg.

Table IV summarizes some of these results. We note, for example, that band *F* in NaF:Mg has an intensity ratio of 0.083 at 300 K. This value is considerably larger than obtained either with a linear dipole moment or with that of Werner, Rosmus, and Reinsch. In this case we find that agreement with experimental intensity ratios using the Sage expression [Eq. (11)] obtains if $r^*=0.858$ Å is used. Here we are in a situation where the transition strength of the fundamental is small and is decreasing with increasing r^*, while that of the overtone is relatively large and is increasing with increasing r^*. Thus, a small

TABLE IV. Experimental (at 300 K) and theoretical overtone-to-fundamental intensity ratios for several bands in NaF:Mg. Theoretical values have been obtained with both a "linear" dipole moment [Eq. (10)] and a "Werner" computed dipole moment (Ref. 17).

Band	Experimental	Theoretical	
		Linear	Werner
A	0.050	0.0226	0.001 38
C	0.015	0.0220	0.001 61
D	0.014	0.0239	0.000 84
F	0.083	0.0239	0.000 84

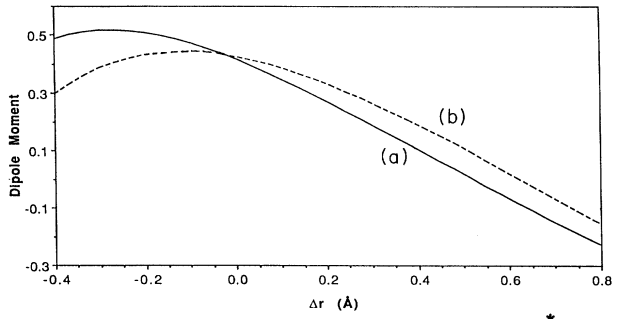

FIG. 2. Two "Sage functions" (Ref. 20), $kre^{-r/r^*}+\text{const.}$ Curve (a) is chosen to fit the computed dipole moment of Werner, Rosmus, and Reinsch (Ref. 17), while curve (b) yields the experimental intensity ratio for band F in NaF:Mg at 300 K. Δr equals $r-r_e$, where $r_e=0.973$ Å.

change in r^* can yield a large change in the ratio.

Figure 2 illustrates two "Sage functions" [Eq. (11)]. Shown is such a function chosen to fit the dipole moment of Werner, Rosmus, and Reinsch and another function which yields the experimental ratio for band F at 300 K.

Figure 3(a) gives the computed $\log_{10}(I_{02}/I_{01})$ versus r^* for some typical values of input parameters. This clearly shows how, in the region r^* around 0.7 Å, the intensity ratio is small and, in fact, becomes zero, and how a large value of r^* is required for the ratio to exceed that predicted by a linear dipole moment variation (shown by the horizontal line). Figure 3(b) shows how I_{01} varies with r^* by a plot of $\log_{10}(I_{01})$ versus r^*, normalized to 1 at $r^*=0.6$ Å.

At this point we can only speculate as to why the electrical anharmonicity is so different from that predicted (and observed) for free OH^-. We note that, for the free molecule, the dipole moment curves are very different for different charge states.[17] If OH^- in the crystal is slightly less ionic than free OH^-, the dipole moment is likely to be rather different as well, in a way which would tend to increase r^* as needed to improve agreement with experiment.

We note as well that, in the crystal, the OH^- defects which we are analyzing are generally in regions of large electric fields, and that neighboring halogen ions are very polarizable. Both of these features would be expected to affect the OH^- dipole moment variation with separation.

D. Other OH^- data

Forster, Kapphan, and Wohlecke[26] have measured the fundamental and the overtone of OH^- and OD^- in

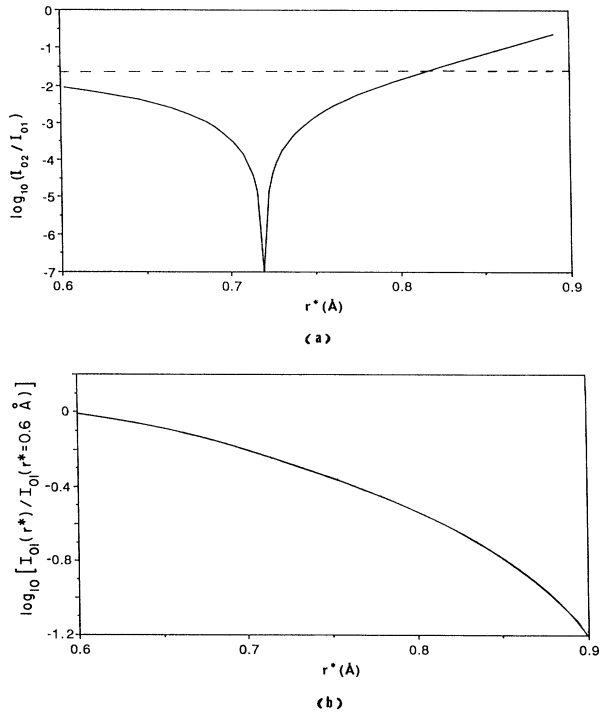

FIG. 3. (a) The computed intensity ratio I_{02}/I_{01} vs r^*, on a $\log_{10}$ scale, using the Sage dipole moment function (Ref. 20) and Morse potential eigenfunctions with the O-H separation $r_e=0.963$ Å, $x_e=0.023\,53$, and $\beta=2.242\,95$ Å^{-1}. The horizontal dashed line is the value obtained for a dipole moment proportional to separation [Eq. (10)]. (b) Computed fundamental intensity I_{01} vs r^*, on a $\log_{10}$ scale, with I_{01} normalized to 1 at $r^*=0.6$ Å. The same Sage function and parameters are used as in (a).

$LiNbO_3$. They analyzed three bands, labeled A, B, and C, on the basis of a free diatomic anharmonic oscillator. This analysis was generally successful, although it predicts somewhat different values of the spectroscopic parameters depending on whether they were obtained from isotope shifts or overtones.

We have reanalyzed the data of Forster, Kapphan, and Wohlecke using the techniques of Sec. II B. Namely, we use Eqs. (7) and (8) to obtain ω_e^H and x_e^H and Eq. (9) to obtain the reduced-mass ratio ρ. We then use a linear spring model with Nb adjacent to O and a variable Nb-O force constant to calculate ρ, which, in turn, yields the O-D overtone wave number in agreement with experiment (to within the stated uncertainties in measurement). The results are shown in Table V. We note that the O-

TABLE V. Wave numbers (in cm^{-1}) for the OH^- fundamental ΔG_{10} and harmonic ΔG_{20} and the OD^- fundamental ΔG_{10}^D and harmonic ΔG_{20}^D, determined experimentally (Ref. 26), and calculated values of ω_e^H (in cm^{-1}) from Eq. (7), x_e^H from Eq. (8), and ρ from Eq. (9), for several ir bands in $LiNbO_3$. Also listed are values of k_{OL}, the O-lattice force constant (as a fraction of the O-H value), which provide best fits to the data.

Band	ΔG_{10}	ΔG_{20}	ΔG_{10}^D	ΔG_{20}^D	ω_e^H	$100x_e^H$	ρ	k_{OL}
A	3483	6778	2575	5050	3671.0	2.561	0.5309	0.305
B	3529	6881	2606	5121	3706.0	2.388	0.5308	0.276
C	3501	6829	2589	5081	3674.0	2.354	0.5326	0.612

TABLE VI. Wave numbers (in cm^{-1}) for the OH^- fundamental ΔG_{10} and harmonic ΔG_{20} and the OD^- fundamental ΔG_{10}^D, determined experimentally (Ref. 27), and calculated values of ω_e^H (in cm^{-1}) from Eq. (7), x_e^H from Eq. (8), and ρ from Eq. (9), for ir bands in CsCl and CsBr. Also listed are values of k_{OL}, the O-lattice force constant (as a fraction of the O-H value) which provide best fits to the data.

Band	ΔG_{10}	ΔG_{20}	ΔG_{10}^D	ω_e^H	$100x_e^H$	ρ	k_{OL}
CsCl	3601.5	7032	2656	3772.5	2.267	0.5301	0.140
CsBr	3580.4	6987	2643	3754.2	2.315	0.5308	0.293

Nb force constants are of order 0.3–0.6 that of O-H, similar to values obtained for other cases.

Krantz and Luty,[27] as part of an extensive series of measurements on vibrational and rotational dynamics of OH^- and OD^- in cesium halides, have presented fundamental and overtone wave numbers for OH^- and fundamental wave numbers for OD^- in CsCl and CsBr. Unlike some cases discussed above, these defects are simple substitutional ions, presumably without divalent cations or vacancies nearby. Krantz and Luty have also measured the transition strength ratios I_{02}/I_{01} for the OH^- defects. They have noted the existence of both mechanical and electrical anharmonicity in these defects and have obtained spectroscopic parameters.

Table VI gives the results of our analysis of the Krantz-Luty data, using the methods of Sec. III B. Equations (7)–(9) are used to obtain ω_e, x_e, and ρ, and a linear spring model with variable Cs-O force constant is used to calculate ρ. The computed Cs-O force constants are again found to be a few tenths of the O-H force constant.

Krantz and Luty found the transition strength ratio I_{02}/I_{01} to equal 0.000 45 for CsCl and 0.0033 for CsBr. Both of these are substantially smaller than x_e, indicating significant electrical anharmonicity. Our calculations using the dipole moment expression for OH^- of Werner, Rosmus, and Reinsch[17] predict a ratio of 0.0011 for CsCl and 0.0010 for CsBr. Varying the Sage parameter r^*, we find agreement with experiment for $r^*=0.693$ or 0.735 Å for CsCl, and $r^*=0.651$ or 0.762 Å for CsBr. These Sage parameters are not substantially different from that appropriate for free OH^-. Again, the ratio I_{02}/I_{01} is sensitive to small changes in this range, as shown in Fig. 3. These small changes may be associated with the presumed off-centeredness of the OH^- ion.

IV. SUMMARY

The spectroscopy of *X*H-containing defects is capable of yielding a rich variety of phenomena, some of which are very sensitive to the nature of the defect. As noted, in particular, in the case of OH^- in insulating crystals, measurements of fundamental and overtone positions and strengths, and isotope shifts, reveal some surprising results.

An analytical technique based on a Morse potential for the diatomic system, modified to account for coupling of O to the environment, may be used to treat such data. The fundamental and overtone transition strengths reveal the existence of large electrical anharmonicities. While in some cases (e.g., the simple substitutional OH^- in CsCl and CsBr) an electric-dipole moment expression close to that obtained by Werner, Rosmus, and Reinsch[17] for diatomic OH^- seems appropriate, in other cases (e.g., OH^- associated with one or more Mg^{2+} ions and cation vacancies in LiF and NaF), the required dipole moment expression is substantially different from that obtained for diatomic OH^-, apparently as a result of environmental effects associated with these complex defects.

ACKNOWLEDGMENTS

The authors are indebted to Dr. István Földvári of the Crystal Physics Laboratory of the Hungarian Academy of Science (Budapest) for supplying the LiF and NaF samples. Discussions with Lehigh colleagues, particularly Dr. Gary DeLeo and Dr. Michael Stavola, were very helpful, as were the detailed comments of Dr. Fritz Luty of the University of Utah on this work.

APPENDIX

We consider a semi-infinite linear array of masses and springs. All the springs are identical (k), and all the masses are the same (M) except for that on the end (m). The normal modes are the solutions of the determinant equation

$$\text{Det}\begin{bmatrix} -m\omega^2+k & -k & 0 & 0 & 0 & \cdots \\ -k & -M\omega^2+2k & -k & 0 & 0 & \cdots \\ 0 & -k & -M\omega^2+2k & -k & 0 & \cdots \\ 0 & 0 & -k & -M\omega^2+2k & -k & \cdots \\ \vdots & \vdots & \vdots & \vdots & \vdots & \ddots \end{bmatrix} \equiv \text{Det}\mathcal{M}=0 \, . \tag{A1}$$

Suppose there are N heavy masses, where N will become large. We call $\mathrm{Det}_N\mathcal{M}$ the $N\times N$ portion of Eq. (A1) corresponding to those heavy masses. We likewise define $\mathrm{Det}_{N-1}\mathcal{M}$ to be the $(N-1)\times(N-1)$ determinant of $N-1$ of the heavy masses, etc. Then Eq. (A1) may be written as

$$(-m\omega^2+k)\mathrm{Det}_N\mathcal{M}-k^2\mathrm{Det}_{N-1}\mathcal{M}=0 \quad \text{(A2)}$$

or

$$-m\omega^2+k=k^2/(\mathrm{Det}_N\mathcal{M}/\mathrm{Det}_{N-1}\mathcal{M}) . \quad \text{(A3)}$$

We then note that the heavy-mass determinant may be written

$$\mathrm{Det}_N\mathcal{M}=(-M\omega^2+2k)\mathrm{Det}_{N-1}\mathcal{M}-k^2\mathrm{Det}_{N-2}\mathcal{M} , \quad \text{(A4)}$$

$$\mathrm{Det}_{N-1}\mathcal{M}=(-M\omega^2+2k)\mathrm{Det}_{N-2}\mathcal{M}-k^2\mathrm{Det}_{N-3}\mathcal{M} , \quad \text{(A5)}$$

etc. These relations may be used to write the right-hand side of Eq. (A3) in recursive form, and in the limit, as N goes to infinity, the right-hand side $\mathcal{R}_N$ may be expressed as

$$\mathcal{R}_N=k^2/(-M\omega^2+2k-\mathcal{R}_N) . \quad \text{(A6)}$$

We may then solve for $\mathcal{R}_N$, substitute the expression into Eq. (A3), and find the expression for ω^2 given in Eqs. (1) and (2). Similar logic may be used to treat extensions of this model in which force constants or heavy masses are not all the same.

[1]B. Wedding and M. V. Klein, Phys. Rev. **177**, 1274 (1969).

[2]M. V. Klein, B. Wedding, and M. A. Levine, Phys. Rev. **180**, 902 (1969).

[3]R. C. Newman, in *Festkörperprobleme XXV, Advances in Solid State Physics,* edited by P. Grosse (Vieweg, Braunschweig, 1985), p. 605.

[4]J. I. Pankove and N. M. Johnson, *Hydrogen in Semiconductors* (Academic, New York, 1991).

[5]J. B. Bates and R. A. Perkins, Phys. Rev. B **16**, 3713 (1977).

[6]R. Capelletti, W. Beall Fowler, G. Ruani, and L. Kovacs, Cryst. Latt. Defects Amorph. Mater. **16**, 189 (1987).

[7]M. S. Burberry and A. C. Albrecht, J. Chem. Phys. **70**, 147 (1979).

[8]J. S. Hutchinson, W. P. Reinhardt, and J. T. Hynes, J. Chem. Phys. **79**, 4247 (1983).

[9]A. Lami and G. Villani, J. Chem. Phys. **88**, 5186 (1988).

[10]A. W. Tarr and F. Zerbetto, Chem. Phys. Lett. **154**, 273 (1989).

[11]R. Barrio, R. J. Elliott, and M. F. Thorpe, J. Phys. C **16**, 3425 (1983).

[12]R. S. Leigh and R. C. Newman, Semicond. Sci. Technol. **3**, 84 (1988).

[13]R. C. Newman, Semicond. Sci. Technol. **5**, 911 (1990).

[14]P. Dumas, Y. J. Chabal, and G. S. Higashi, Phys. Rev. Lett. **65**, 1124 (1990).

[15]P. M. Morse, Phys. Rev. **34**, 57 (1929).

[16]J. E. Rosenthal, Proc. Natl. Acad. Sci. U.S.A. **21**, 281 (1935).

[17]H. -J. Werner, P. Rosmus, and E. -A. Reinsch, J. Chem. Phys. **79**, 905 (1983).

[18]A. W. Tarr, D. J. Swanton, and B. R. Henry, J. Chem. Phys. **85**, 3463 (1986).

[19]H. S. Heaps and G. Herzberg, Z. Phys. **133**, 48 (1952).

[20]Martin L. Sage, Chem. Phys. **35**, 375 (1978).

[21]Y. V. Gorelkinskii and N. N. Nevinnyi, Pis'ma Zh. Tekh. Fiz. **13**, 105 (1987) [Sov. Tech. Phys. Lett. **13**, 45 (1987)]; V. A. Gordeev, Yu. V. Gorelkinskii, R. F. Konopleva, N. N. Nevinnyi, Yu. V. Obukhov, and V. G. Firsov (unpublished).

[22]J. Isoya, J. A. Weil, and L. E. Halliburton, J. Chem. Phys. **74**, 5436 (1981).

[23]J. Hanley, R. DiSipio, M. Ludinsky, H. Sun, I. Veloarisoa, and X. Wang (unpublished).

[24]G. Herzberg, *Molecular Spectra and Molecular Structure I. Spectra of Diatomic Molecules,* 2nd ed. (Van Nostrand Reinhold, New York, 1950).

[25]R. Capelletti, E. Colombi, R. Fieschi, A. Gainotti, W. B. Fowler, and I. Foldvari, Rad. Effects Defects Solids (to be published).

[26]A. Forster, S. Kapphan, and M. Wohlecke, Phys. Status Solidi B **143**, 755 (1987).

[27]Matthias Krantz and Fritz Luty, Phys. Rev. B **37**, 7038 (1988).